

Available online at [www.sciencedirect.com](http://www.sciencedirect.com)

**jmr&t**  
Journal of Materials Research and Technology  
[www.jmrt.com.br](http://www.jmrt.com.br)



## Original Article

# A study surface integrity of aluminum hybrid composites during milling operation

P. Rasagopal<sup>a,\*</sup>, P. Senthilkumar<sup>a</sup>, G. Nallakumarasamy<sup>b</sup>, S. Magibalan<sup>a</sup>

<sup>a</sup> Department of Mechanical Engineering, K.S.R. College of Engineering, Tiruchengode 637215, Tamil Nadu, India

<sup>b</sup> Department of Mechanical Engineering, Excel Engineering College, Komarapalayam, Tamil Nadu, India

## ARTICLE INFO

## Article history:

Received 25 December 2019

Accepted 3 March 2020

Available online xxx

## Keywords:

Aluminum metal matrix composites

Optimization of machining

parameters

Taguchi method

Surface roughness

Reinforcement of metal matrix

composites

## ABSTRACT

In this article, the effects of machining parameters on surface roughness and cutting force on hybrid aluminum metal matrix composites were investigated. Three reinforced composites were made by adding three compositions of SiC and boron carbide (B<sub>4</sub>C) by stir-casting method. Machining was performed on fabricated composite material using milling operation with different cutting parameters. The roughness of the machined surfaces was determined by the Mitutoyo SurfTest SV-2100 Column-type surface roughness tester. Cutting forces in the y-direction was measured. Further, the results were optimized and analyzed by Taguchi method. The obtained experimental results demonstrate that the most important machining parameters are feed rate, cutting speed and depth of cut on surface roughness, and cutting force.

© 2020 The Authors. Published by Elsevier B.V. This is an open access article under the CC BY-NC-ND license (<http://creativecommons.org/licenses/by-nc-nd/4.0/>).

## 1. Introduction

In the current scenario, advancements in materials are being promoted as real-time applications require high-strength, low-weight materials. Aerospace and automobile industries are the major consumers of lightweight and high-strength materials [1]. Increased strength-to-weight ratio brings many advantages for their applications such as reduced mass, reduced material requirements, and increased load-carrying capacity [1]. Thus, these materials have attracted significant attention. For the increased performance requirements of materials, such as high hardness, resistant to wear, and resistance to corrosion, instead of conventional materials, metal matrix composites (MMCs) are utilized [2]. MMCs are pre-

pared using continuous metallic matrix and reinforcements. The reinforcements may have continuous and discontinuous phases and be in the form of whiskers, fibers, or particulates. They can be metallic or ceramics. Studies have been conducted on MMCs regarding their production methods and estimation of their properties. Particulate metal matrix composites (PMMCs) are of interest these days because of their excellent engineering properties and potential of use in a number of applications [3].

Among the various available MMCs, aluminum (Al) alloy-based MMCs are extensively utilized because of their high specific strength, fatigue resistance, stiffness, capability of withstanding relatively high temperatures, and low cost. Specifically, particulate-reinforced aluminum alloy composites are gaining attention from researchers. They have been used to manufacture various automobile components including cylinder lining, pistons, drive shafts, and frames for automobiles [4]. One of the major problems that arise

\* Corresponding author.

E-mail: [rasagopalksrcemech@gmail.com](mailto:rasagopalksrcemech@gmail.com) (P. Rasagopal).

<https://doi.org/10.1016/j.jmrt.2020.03.008>

2238-7854/© 2020 The Authors. Published by Elsevier B.V. This is an open access article under the CC BY-NC-ND license (<http://creativecommons.org/licenses/by-nc-nd/4.0/>).

**Table 1 – Elements of Al 7075.**

Element	Composition of Al 7075 (%)
Zinc (Zn)	5.4
Copper (Cu)	1.42
Manganese (Mn)	0.12
Magnesium (Mg)	2.42
Ferrite (Fe)	0.42
Chromium (Cr)	0.21
Aluminum (Al)	Rest

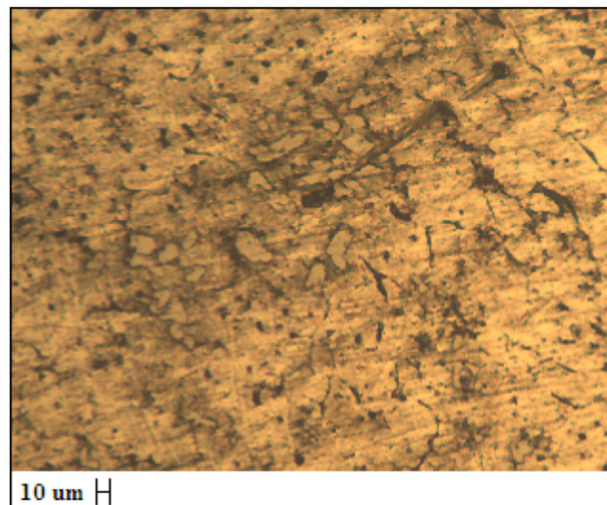
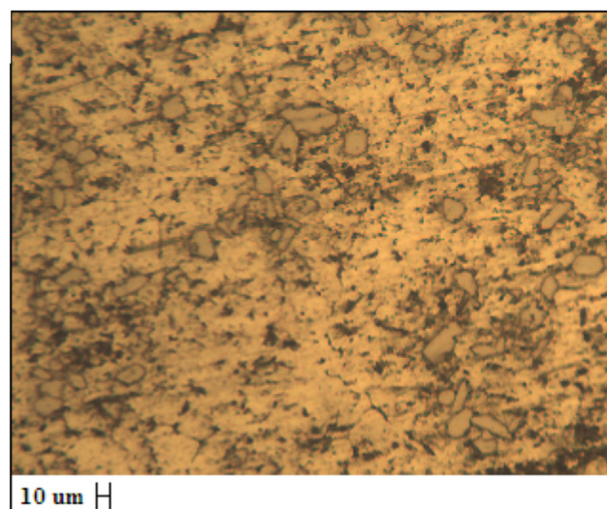
**Table 2 – Process parameters and their levels.**

Factor	Notation	Unit	Level		
			Level 1	Level 2	Level 3
Cutting speed	S	rpm	1000	1500	2000
Feed	F	mm/min	30	60	90
Depth of cut	D	mm	1	1.5	2

while working with these composite materials is machining. Reduced tool life, diffusion, and dimensional instability are the major issues faced due to increased hardness and thermal loads during machining of these materials. Besides, surface roughness is also a quality concern of products manufactured using aluminum alloy-based PMMCs. Finding the most effective machining parameter and optimizing it could be the best way to improve the quality of product with regard to surface roughness [5]. In this article, the parameters that affect the product surface finish and cutting force were studied. The preparation of specimen and setup are also discussed.

Preparation of MMCs is done through several techniques including casting and powder metallurgy. Though casting is generally used, there are challenges associated with it. One of those challenges include homogeneous distribution of reinforcements, which has direct impact on the quality and properties of the composite [6]. Stir-casting technique is followed to overcome the challenge in MMC preparation. Many authors have investigated the influence of process parameters and percentage of compositions on the quality of the composite, life of the tool, and machinability. Adding silicon carbides (SiC) to aluminum from 5% to 15% by weight increases toughness and hardness considerably [7]. Pawar and Utpat [8] prepared a composite by adding SiC in aluminum at various levels, from 2.5% to 10% by mass. On the basis of the mechanical tests, though tensile strength showed a different trend, the toughness and hardness are the properties that showed enhancement. Added to this, Seeman et al. [3] increased the amount of silicon carbide up to 20% and evaluated the machinability of the composite. However, the core mechanical properties such as toughness, harness, wear resistance, and thermal stability were increased in MMCs. It is a big challenge to achieve improvement in terms of surface roughness during machining.

Many investigations have been conducted on machining of aluminum alloy-based MMCs by various researchers. The

(a) Al 7075 (1% SiC + 1% B<sub>4</sub>C),(b) Al 7075 (3% SiC + 3% B<sub>4</sub>C)**Fig. 1 – Microstructure of (a) Al 7075 (1% SiC + 1% B<sub>4</sub>C), (b) Al 7075 (3% SiC + 3% B<sub>4</sub>C).**

types of machining include turning [9], grinding [10,11], and milling [12]. But studies on the optimization of milling parameters for machining aluminum alloy-based MMCs are few in the literature. Most of the available reports reveal that machining of aluminum alloy-based composites provides lower surface integrity but, in contrast, Reddy et al. [13] have compared the surface integrity of nonreinforced aluminum alloys with reinforced aluminum alloys after milling. Aluminum alloy-based PMMCs ensure better machining compared to others. Kuram and Ozcelik [14] formulated a four-stage method to investigate optimization of parameters during milling. The methods include experimental modeling followed by mono- and multi-objective optimization. To get optimized cutting parameters, most of the researchers use Taguchi technique [15,16]. It enhances the quality of machined surface as well as the economical machining operations. Hence, optimization of machining parameters during machining of MMCs is still the need of hour. This article aims to optimize machining

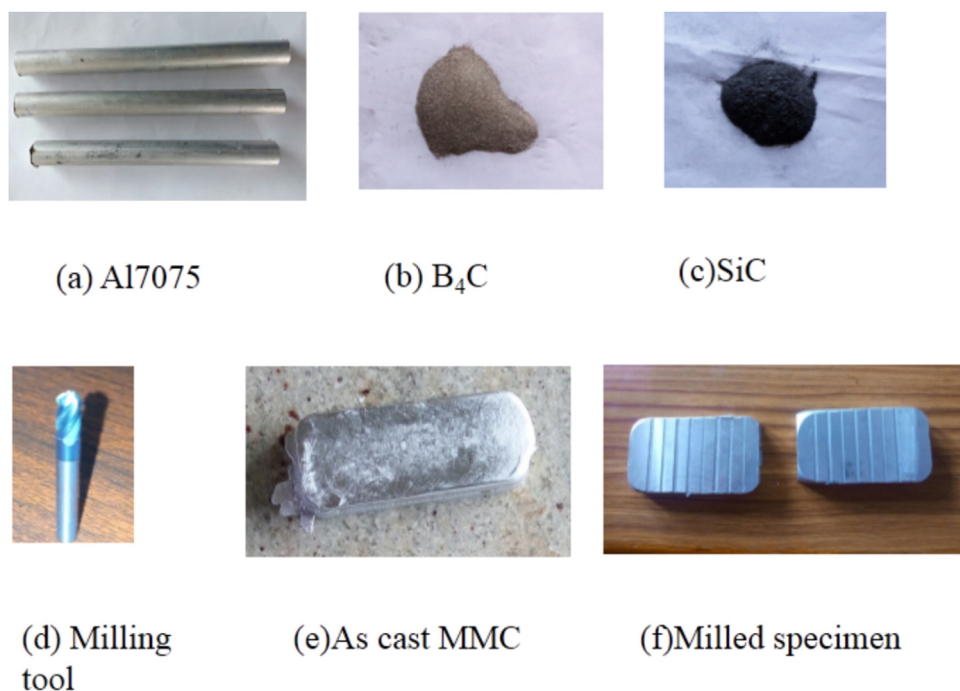


**Fig. 2 – Materials and tools for MMC milling.**

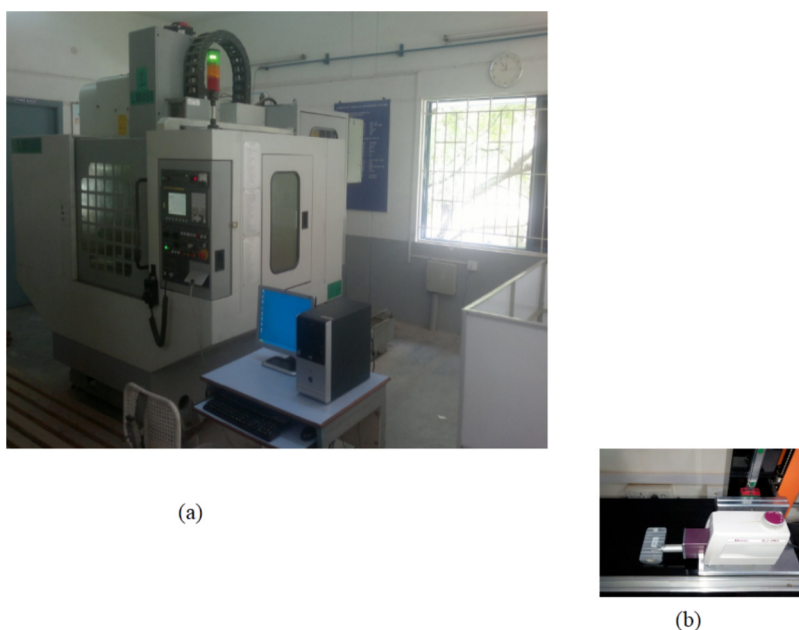


**Fig. 3 – (a) Experimental setup for milling of rectangular MMCs. (b) Surface roughness measurements.**

parameters for milling operation on Al 7075/SiC/B<sub>4</sub>C hybrid MMCs.

## 2. Materials and methods

Aluminum 7075 hybrid MMCs with 2, 4, and 6wt% SiC and B<sub>4</sub>C were utilized in this investigation. The hybrid aluminum composite reinforced with SiC and B<sub>4</sub>C was prepared by stir-casting route. Cast composites with dimensions of

70 mm × 50 mm × 10 mm were cut. Table 1 displays the chemical composition of aluminum 7075 alloy. Fig. 1(a) and (b) demonstrates the microstructure of as-prepared composite samples of aluminum 7075 with, respectively, 2% and 6% SiC and B<sub>4</sub>C particles. A careful analysis of the micrographs shows uniform distribution of SiC and B<sub>4</sub>C particles in the aluminum matrix. Fig. 1(b) demonstrates a minor agglomeration of SiC and B<sub>4</sub>C particles in the 6% reinforcement MMCs compared to 2% MMCs. Fig. 2 shows Al 7075 rods, SiC and B<sub>4</sub>C parti-

**Table 3 – Experimental design.**

Std. order	Run order	Cutting speed (rpm)	Feed (mm/min)	Depth of cut (mm)
18	1	1000	30	1.0
9	2	1000	30	1.5
16	3	1000	30	2.0
26	4	1000	60	1.0
12	5	1000	60	1.5
6	6	1000	60	2.0
3	7	1000	90	1.0
15	8	1000	90	1.5
8	9	1000	90	2.0
24	10	1500	30	1.0
25	11	1500	30	1.5
22	12	1500	30	2.0
17	13	1500	60	1.0
21	14	1500	60	1.5
20	15	1500	60	2.0
19	16	1500	90	1.0
4	17	1500	90	1.5
5	18	1500	90	2.0
11	19	2000	30	1.0
14	20	2000	30	1.5
10	21	2000	30	2.0
23	22	2000	60	1.0
13	23	2000	60	1.5
7	24	2000	60	2.0
1	25	2000	90	1.0
27	26	2000	90	1.5
2	27	2000	90	2.0

cles, a cast aluminum block, a milling tool, and a machined specimen.

### 3. Experimental study details

The experiment was conducted on a CNC milling machine for cutting 25-mm-long slots on 10-mm-thick test specimens. Fig. 3(a) demonstrates the milling machine used in this study. Fig. 3(b) displays the milled workpiece. The average surface roughness ( $R_a$ ) of the milled samples was calculated using a Talysurf surface roughness measurement equipment. The machined surfaces were examined using a LEO-32 SEM (scanning electron microscope). Table 3 shows the parameters utilized for doing experiments. Each test was conducted three times and the average of the obtained results was considered for further study. Table 2 shows the process parameters used in the experiments along with their levels. Table 3 shows the L27 orthogonal array of Taguchi method.

### 4. Results and discussion

#### 4.1. Effects of cutting parameters on surface roughness

Fig. 4(a)–(c) shows the effect of cutting parameters on surface roughness while machining hybrid MMC. When the cutting

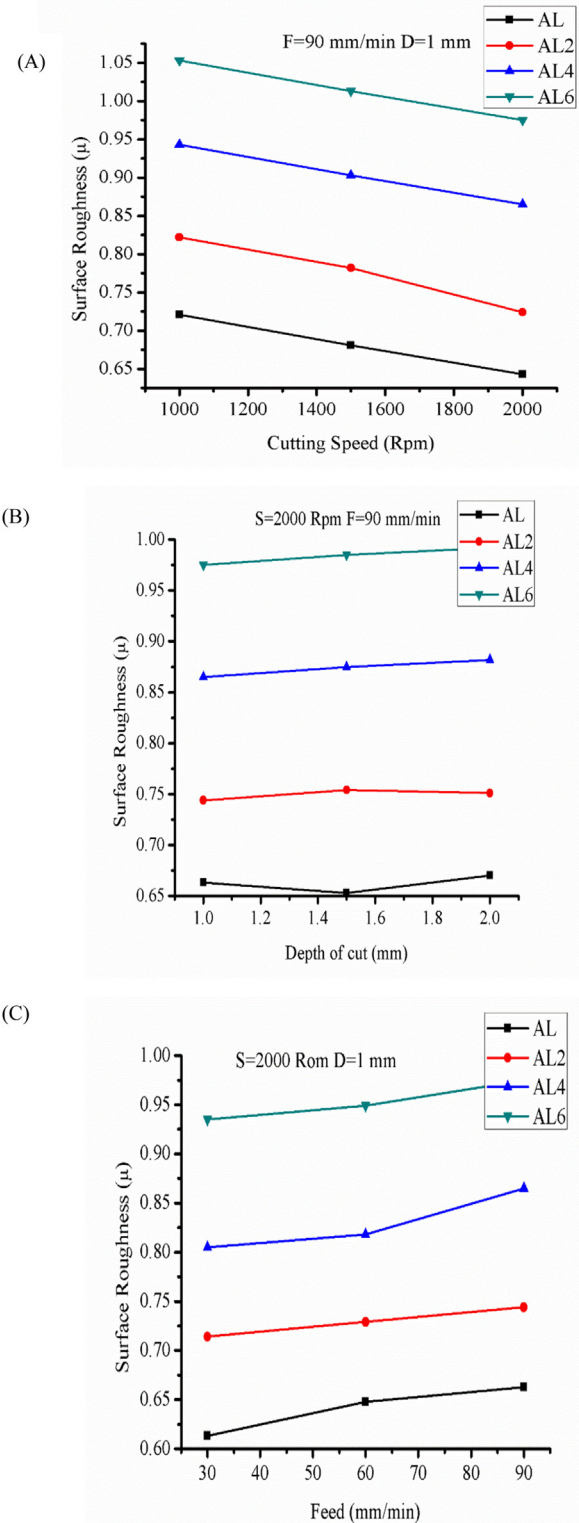


**Fig. 4 – Effects of (a) cutting speed, (b) feed, and (c) depth of cut on surface roughness.**

speed increases, the surface roughness improves. This may be due to softening of material at high speeds. The minimum  $R_a$  was observed at high machining speed and lowest feed rate. This was attributed to high build-up edge (BUE) formation at low cutting speeds on the cutting insert during milling. The previous and latest studies specify that high cutting temperatures are produced at high cutting speed and high feed rate [17,18]. The quality of surface is decreased on increasing the cutting feed from 30 to 90 mm/min (Fig. 4(a)–(c)).

Faster feed rates demonstrate a detrimental effect on the machined surface for machining of both composites. This may be accredited to high vibration and high cutting temperatures in the machining area. The machining temperature rises at greater feed rates, leading to softening of the aluminum matrix in the composite morphology.

#### 4.2. Effect of cutting parameters on force

Fig. 5(a)–(c) shows the difference in cutting forces for Al 7075 and Al/SiC/B<sub>4</sub>C hybrid composite with 2%, 4%, and 6% reinforcement in equal proportion for variable cutting speed, keeping feed and depth of cut constant at 90 mm/min and 1 mm, respectively. It can be seen from the figure that the cutting force components for the Al 7075 alloy were more than those of the reinforced specimens. It can also be observed that the cutting force components decrease as the cutting speed increases and decrease as the percentage of reinforcement increases. The decrease in cutting forces was seen with an increase in the cutting speed, which could be due to thermal softening of the workpiece and this agrees well with the studies published by Gallab et al. [14]. Fig. 5(a)–(c) displays the cutting force components at different feed rates keeping the cutting speed and depth of cut constant at 2000 rpm and 1 mm, respectively, for base material as well as the hybrid specimens with varying reinforcement. It was observed that all cutting force components increase as the feed rate increases and decrease as the reinforcement weight percentage increases.

The cutting force components were observed to increase as the feed rate increased, which could be ascribed to the increased friction between the cutting edge and the workpiece. The reduction in cutting force components with the increase in reinforcement may be attributed to the increase in porosity. During preparation of composites, porosity is a common phenomenon that cannot be fully avoided but can be minimized. The increase in depth of cut also influences the cutting force. The increase in cut depth increases the resistance of the material. This makes the cutting tool to offer more force to remove material.

#### 4.3. The machined surface characteristics

Workpiece surfaces were also analyzed by SEM and some their examples are shown in Fig. 6(a)–(d). It is clearly observed from the surface texture that it is the defined step over traces. It is observed from Fig. 6(a) and (b) that workpiece surfaces has the accumulations of plastically deformed workpiece material because of high ductility of aluminum material. The accumulation of smeared material on the main ridges can also be identified as reported in the literature. It was noticed that during the machining process the residual smeared material

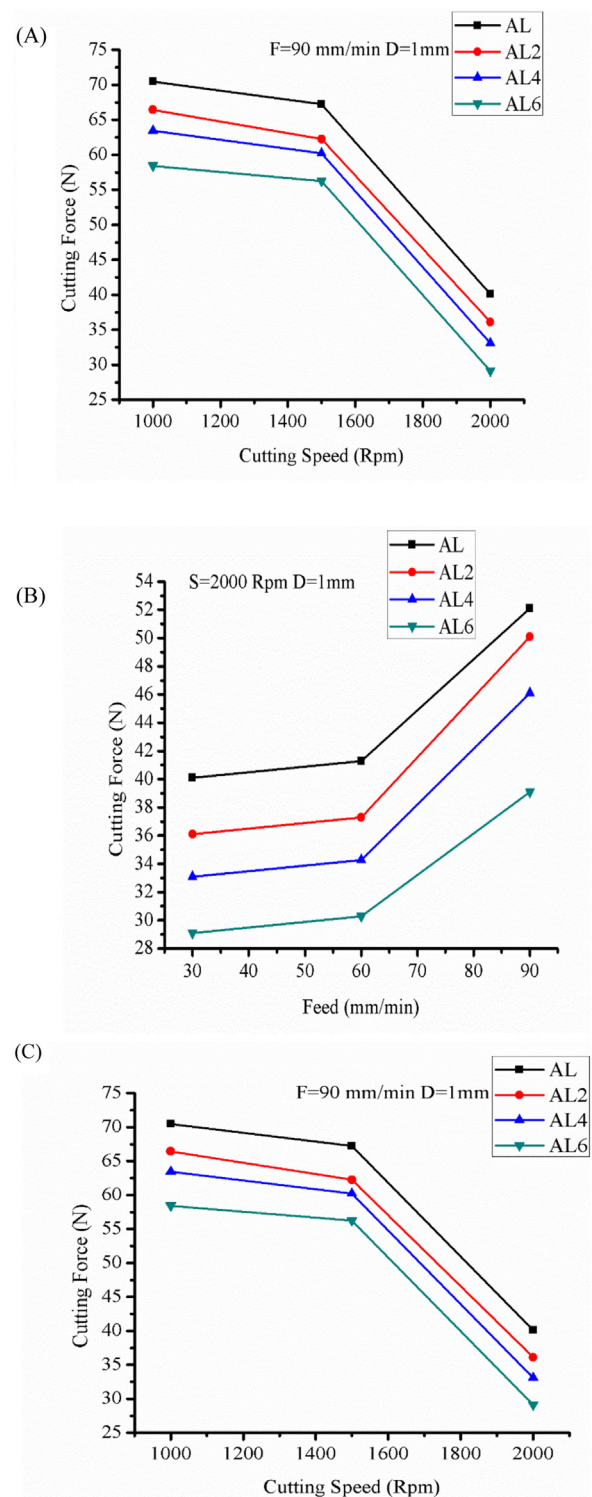
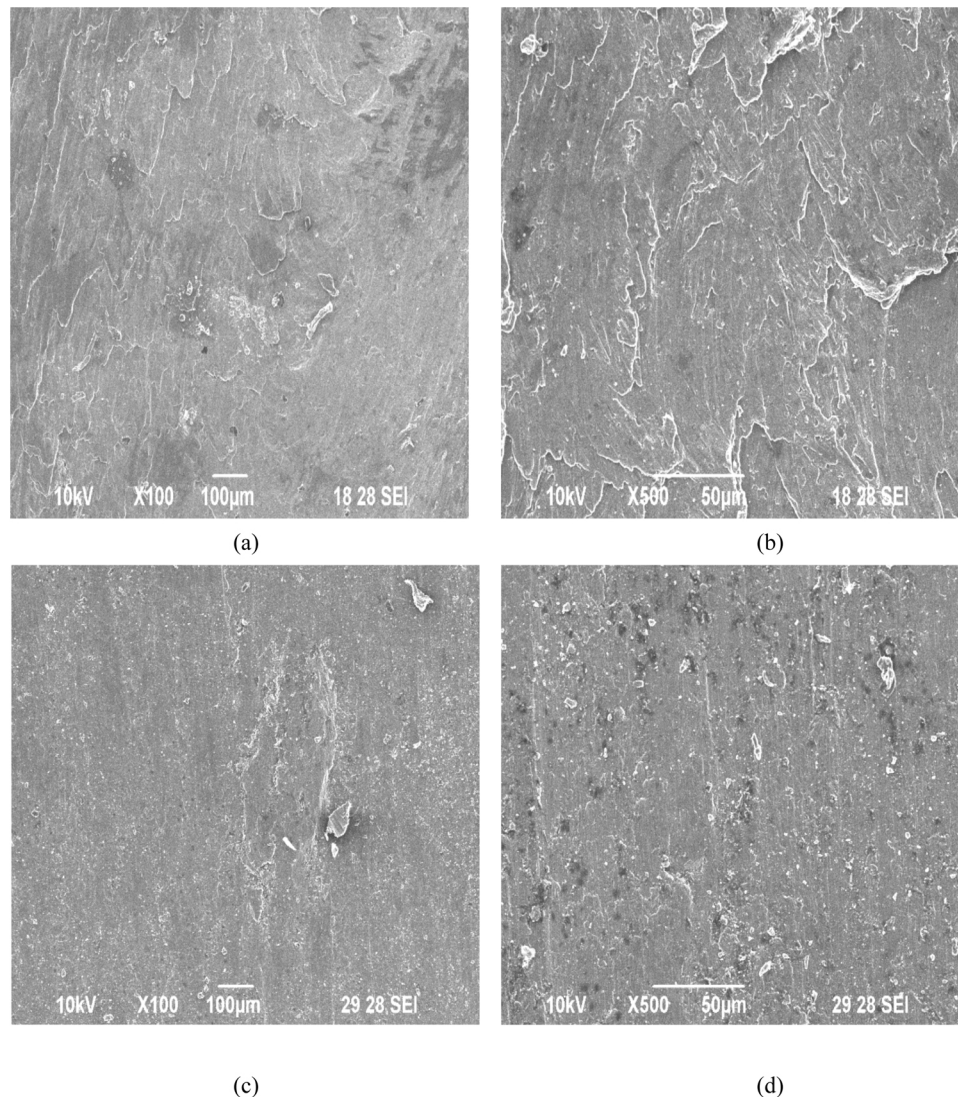


Fig. 5 – Effects of (a) cutting speed, (b) feed, and (c) depth of cut on force.

on the machined surface formed a poor quality of the surface during the milling of Al 7075/SiC/B<sub>4</sub>C composites. Rather than cutting, a part of the softened matrix was swept and moved across the machined surface, and the other part of the softened workpiece was stuck to the cutting insert as a BUE formation [19].



**Fig. 6 – SEM image of the machined surface.**

#### 4.4. ANOVA for surface roughness

Table 4(a)–(d) shows analysis of variance (ANOVA) criteria for surface roughness. Among the three input criteria, the contribution of cutting speed is higher, influencing the surface roughness. For higher reinforcement MMCs, the values of cutting speed, feed, and depth of cut are 43.38%, 35.11%, and 7.61%, respectively.

#### 4.5. ANOVA for force

Table 5(a)–(d) displays the ANOVA parameters for force. The F ratios for cutting speed, feed, and depth of cut are higher than those from statistical tables. The P-values obtained from ANOVA for these criteria are less than 0.05. Therefore, it can be deduced that these criteria influence the force significantly. The force is mainly influenced by cutting speed. The contribution of cutting speed, feed, and depth of cut in force of 100% alloy is 63.3%, 4.4%, and 4.4%, respectively, whereas for MMC

with 6%SiC + B<sub>4</sub>C the contribution of cutting speed, feed and depth of cut in force is 67.5%, 3.4%, and 3.8%, respectively.

#### 4.6. Regression analysis

The below given regression equations for surface roughness and force were acquired from regression analysis using MINITAB program. Tables 6 and 7 display different regression coefficients for predicting surface roughness and force of various MMCs machined with a milling machine. The mathematical model is beneficial in forecasting the machining response of milling process during machining of hybrid MMCs. Eqs. (1) and (2) yield the mathematical association of different input parameters on the output parameters. The machining parameters may be chosen for practical works in manufacturing industries from the model developed in this study. For the regression analysis, R<sup>2</sup> values have also been provided alongside:

$$SR = a + bxS + cxF + dxD + ex(S * S) + fx(S * F) + gx(S * D)$$

**Table 4 – Results of ANOVA for surface roughness.**

Parameter	DF	Seq.SS	Adj.SS	Adj.MS	F	P	% Contribution
<i>(a) Results of ANOVA for surface roughness-100% alloy</i>							
S (rpm)	2	0.008422	0.008422	0.004211	39.14	0	32.87
F (mm/min)	2	0.013192	0.013192	0.006596	61.31	0	51.49
D (mm)	2	0.000854	0.000854	0.000427	3.97	0.064	3.33
SF	4	0.001735	0.001735	0.000434	4.03	0.044	6.77
SD	4	0.000146	0.000146	3.66E-05	0.34	0.844	0.57
FD	4	0.000411	0.000411	0.000103	0.96	0.481	1.61
Error	8	0.000861	0.000861	0.000108			3.36
Total	26	0.025621					100.00
<i>(b) Results of ANOVA for surface roughness-Al 7075 (1% SiC + 1% B<sub>4</sub>C)</i>							
S (rpm)	2	0.016168	0.016168	0.008084	91.81	0	51.03
F (mm/min)	2	0.011065	0.011065	0.005532	62.83	0	34.92
D (mm)	2	0.000793	0.000793	0.000396	4.5	0.049	2.50
SF	4	0.001626	0.001626	0.000407	462.00%	0.032	5.13
SD	4	0.000878	0.000878	0.00022	2.49	0.126	2.77
FD	4	0.00045	0.00045	0.000112	1.28	0.355	1.42
Error	8	0.000704	0.000704	8.81E-05			2.22
Total	26	0.031685					100.00
<i>(c) Results of ANOVA for surface roughness-Al 7075 (2% SiC + 2% B<sub>4</sub>C)</i>							
S (rpm)	2	0.015149	0.015149	0.007575	53.37	0	43.30
F (mm/min)	2	0.011961	0.011961	0.005981	42.14	0	34.19
D (mm)	2	0.003131	0.003131	0.001566	11.03	0.005	8.95
SF	4	0.001729	0.001729	0.000432	3.05	0.084	4.94
SD	4	0.001073	0.001073	0.000268	1.89	0.206	3.07
FD	4	0.00081	0.00081	0.000203	1.43	0.309	2.32
Error	8	0.001135	0.001135	0.000142			3.25
Total	26	0.034989					100.00
<i>(d) Results of ANOVA for surface roughness-Al7075 (3% SiC + 3% B<sub>4</sub>C)</i>							
S (rpm)	2	0.015365	0.015365	0.007682	212.04	0	43.38
F (mm/min)	2	0.012435	0.012435	0.006218	171.6	0	35.11
D (mm)	2	0.002695	0.002695	0.001347	37.19	0	7.61
SF	4	0.002065	0.002065	0.000516	14.25	0.001	5.83
SD	4	0.000262	0.000262	6.54E-05	1.8	0.221	0.74
FD	4	0.002305	0.002305	0.000576	15.9	0.001	6.51
Error	8	0.00029	0.00029	3.62E-05			0.82
Total	26	0.035415					100.00

$$+ hx(F * F) + i(F * D) + jx(D * D) + \dots \quad (1)$$

5% between experimentally obtained values and predicted values by regression model.

$$F = a + bxS + cxF + dxD + ex(S * S) + fx(S * F) + gx(S * D)$$

$$+ hx(F * F) + i(F * D) + jx(D * D) + \dots \quad (2)$$

where S, F, and D are cutting speed, feed rate, and depth of cut, respectively.

After analyzing the contribution of all individual and interaction parameters, the nonsignificant parameters were deleted from the regression equation. Tables 8 and 9 show the coefficient values for the regression equation.

#### 4.7. Confirmation tests

To verify the obtained results from the experiment, a confirmation test was conducted. Table 10 shows the experimental conditions for the confirmation test. Table 11 shows the results of confirmation experimental test for surface characteristics and force. From the table, it can be seen that error is less than

## 5. Conclusions

In this work, the effects of SiC and B<sub>4</sub>C reinforcement to Al 7075 alloy on surface roughness and cutting force during milling were studied in terms of specific parameters such as cutting speed, feed rate, and depth of cut. Hybrid MMCs with different weight fraction of reinforcements SiC and B<sub>4</sub>C were fabricated by stir-casting method. Taguchi L27 orthogonal array with ANOVA was used to optimize machining parameters. From the results of ANOVA, it was found that the cutting speed and feed rate exert the largest effect on the surface roughness. On increasing the cutting speed, the surface roughness decreases and vice versa. When the feed rate increases, the surface roughness increases and vice versa for all the composites. Higher cutting speeds lead to comparative easier separation of the hard SiC and B<sub>4</sub>C particles, resulting in better surface finish. When percentage of reinforcement is increased, the surface roughness worsens. The models for predicting surface roughness and cutting force are useful to

**Table 5 – Results of ANOVA for force.**

Parameter	DF	Seq.SS	Adj.SS	Adj.MS	F	P	% Contribution
<i>(a) Results of ANOVA for surface roughness-100% alloy</i>							
S (rpm)	2	2376.13	2376.13	1188.07	28.26	0	63.30759
F (mm/min)	2	159.16	159.16	79.58	1.89	0.212	4.240524
D (mm)	2	161.32	161.32	80.66	192.00%	0.209	4.298073
SF	4	274.43	274.43	68.61	1.63	0.257	7.31168
SD	4	218.12	218.12	54.53	1.3	0.348	5.811404
FD	4	227.79	227.79	56.95	1.35	0.33	6.069043
Error	8	336.36	336.36	42.04			8.96169
Total	26	3753.31					100
<i>(b) Results of ANOVA for surface roughness-Al 7075 (1% SiC + 1% B<sub>4</sub>C)</i>							
S (rpm)	2	2209.47	2209.47	1104.73	27.81	0	60.9146
F (mm/min)	2	170.7	170.7	85.35	2.15	0.179	4.706161
D (mm)	2	173.99	173.99	86.99	2.19	0.174	4.796866
SF	4	273.54	273.54	68.38	1.72	0.238	7.541437
SD	4	203.83	203.83	50.96	1.28	0.353	5.619548
FD	4	277.79	277.79	69.45	1.75	0.232	7.658609
Error	8	317.84	317.84	39.73			8.762779
Total	26	3627.16					100
<i>(c) Results of ANOVA for surface roughness-Al 7075 (2% SiC + 2% B<sub>4</sub>C)</i>							
S (rpm)	2	2197.89	2197.89	1098.95	27.91	0	61.98555
F (mm/min)	2	186.03	186.03	93.02	2.36	0.156	5.246474
D (mm)	2	161.58	161.58	80.79	2.05	0.191	4.556928
SF	4	230.9	230.9	57.72	1.47	0.298	6.511911
SD	4	223.44	223.44	55.86	1.42	0.312	6.301522
FD	4	230.94	230.94	57.73	1.47	0.298	6.513039
Error	8	315.03	315.03	39.38			8.884571
Total	26	3545.81					100
<i>(d) Results of ANOVA for surface roughness-Al7075 (3% SiC + 3% B<sub>4</sub>C)</i>							
S (rpm)	2	2475.28	2475.28	1237.64	33.08	0	67.49285
F (mm/min)	2	125.9	125.9	62.95	1.68	0.246	3.432884
D (mm)	2	142.66	142.66	71.33	1.91	0.21	3.889875
SF	4	166.29	166.29	41.57	1.11	0.415	4.534188
SD	4	236.09	236.09	59.02	1.58	0.27	6.437408
FD	4	221.96	221.96	55.49	1.48	0.294	6.052129
Error	8	299.29	299.29	37.41			8.160667
Total	26	3667.47					100

**Table 6 – Regression coefficients for surface roughness.**

	Al 7075 with			
	100% alloy	1% SiC + 1% B <sub>4</sub> C	2% SiC + 2% B <sub>4</sub> C	3% SiC + 3% B <sub>4</sub> C
a	0.475759	0.623611	6.41E-01	0.674269
b	3.84E-05	1.84E-05	7.47E-05	0.000121
c	0.003056	0.00225	0.002444	0.003478
d	0.102778	0.113889	0.175444	0.210722
e	-6.44E-09	-8.67E-09	-3.76E-08	-4.62E-08
f	-7.56E-07	-5.89E-07	-7.00E-07	-7.00E-07
g	-1.13E-05	-1.13E-05	1.53E-05	1.67E-06
h	-6.05E-06	-4.81E-06	1.23E-07	-9.88E-06
i	-0.0002	2.22E-05	-0.00037	-0.00026
j	-0.02044	-0.02933	-0.05156	-0.06022
R <sup>2</sup>	96.64%	91.72%	91.75%	90.35%



**Table 7 – Regression coefficients for force.**

	Al7075 with			
	100% alloy	1% SIC + 1% B <sub>4</sub> C	2% SIC + 2% B <sub>4</sub> C	3% SIC + 3% B <sub>4</sub> C
a	7.89083	9.31713	12.3264	-6.0162
b	0.025448	0.018568	0.019846	0.033124
c	0.22788	0.221083	0.153491	0.247935
d	51.8883	50.0083	42.7306	47.4528
e	-1.37E-05	-1.18E-05	-1.29E-05	-1.58E-05
f	6.33E-05	7.94E-05	9.06E-05	3.50E-05
g	-0.00722	-0.00663	-0.00563	-0.0073
h	0.001109	0.001133	0.00138	0.001133
i	-0.23917	-0.25028	-0.23361	-0.23361
j	-7.02667	-6.36889	-4.81333	-5.70222
R <sup>2</sup>	96.64%	97.78%	96.75%	99.18%

**Table 8 – Modified regression coefficients for surface roughness.**

	Al 7075 with			
	100% alloy	1% SIC + 1% B <sub>4</sub> C	2% SIC + 2% B <sub>4</sub> C	3% SIC + 3% B <sub>4</sub> C
a	0.489185	0.700111	0.702963	0.756519
b	1.91E-05	3.39E-05	5.57E-05	8.18E-05
c	0.00305556	0.0014	0.000844444	0.00204444
d	0.102778	0.0982222	0.176444	0.197889
e	-	-8.67E-09	-3.76E-08	-4.62E-08
f	-7.56E-07	-	-	-
g	-1.13E-05	-	-	-
h	-6.05E-06	-4.81E-06	1.23E-07	-9.88E-06
i	-0.0002	-	-	-
j	-0.0204444	-0.0293333	-0.0515556	-0.0602222
R <sup>2</sup>	97.64%	92.72%	93.75%	93.35%

**Table 9 – Modified regression coefficients for force.**

	Al 7075 with			
	100% alloy	1% SIC + 1% B <sub>4</sub> C	2% SIC + 2% B <sub>4</sub> C	3% SIC + 3% B <sub>4</sub> C
a	2.19083	5.91898	8.1875	-9.41435
b	0.029248	0.018568	0.019846	0.033124
c	0.32288	0.357009	0.319046	0.383861
d	51.8883	50.0083	42.7306	47.4528
e	-1.37E-05	-1.18E-05	-1.29E-05	-1.58E-05
f	-	7.94E-05	9.06E-05	3.50E-05
g	-0.00722	-0.00663	-0.00563	-0.0073
h	0.001109	-	-	-
i	-0.23917	-0.25028	-0.23361	-0.23361
j	-7.02667	-6.36889	-4.81333	-5.70222
R <sup>2</sup>	97.00	96.29	96.98	98.84

**Table 10 – Experimental conditions for confirmation test.**

Test	Cutting speed	Feed	Depth of cut
1	1200	40	1.3
2	1300	50	1.6
3	1600	70	1.8

**Table 11 – Confirmation test results.**

	Test no.	Test 1			Test 2			Test 3		
		Reg.	Exp.	Err.	Reg.	Exp.	Err.	Reg.	Exp.	Err.
Surface roughness	100% alloy	0.66	0.64	3.03	0.676	0.666	1.48	0.681	0.654	3.96
	1% SiC + 1% B <sub>4</sub> C	0.769	0.73	5.07	0.78	.76	2.56	0.779	0.747	4.11
	2% SiC + 2% B <sub>4</sub> C	0.887	0.86	3.04	0.903	.87	3.65	0.905	0.89	1.66
	3% SiC + 3% B <sub>4</sub> C	1.000	0.94	6.00	1.02	0.95	6.86	1.02	0.98	3.92
Force	100% alloy	64.5	65.4	-1.40	67	66	1.49	61.7	60.1	2.59
	1% SiC + 1% B <sub>4</sub> C	60.0	59.1	1.50	62.5	61.2	2.08	57.5	56.3	2.09
	2% SiC + 2% B <sub>4</sub> C	56.7	55.4	2.29	59	58	1.69	54.4	53.2	2.21
	3% SiC + 3% B <sub>4</sub> C	52.9	51.2	3.21	55.3	54.3	1.81	49.9	48.1	3.61

identify the optimum parameter setting while machining Al 7075 hybrid MMCs.

### Conflicts of interest

The authors declare no conflicts of interest.

### REFERENCES

- [1] Bakshi SR, Lahiri D, Agarwal A. Carbon nanotube reinforced metal matrix composites—a review. *Int Mater Rev* 2010;55(1):41–64.
- [2] Lin C, et al. Machining and fluidity of 356Al/SiC (p) composites. *J Mater Process Technol* 2001;110(2):152–9.
- [3] Seeman M, et al. Study on tool wear and surface roughness in machining of particulate aluminum metal matrix composite-response surface methodology approach. *Int J Adv Manuf Technol* 2010;48(5–8):613–24.
- [4] El-Gallab M, Sklad M. Machining of Al/SiC particulate metal-matrix composites. Part I. Tool performance. *J Mater Process Technol* 1998;83(1–3):151–8.
- [5] Palanikumar K, Karthikeyan R. Assessment of factors influencing surface roughness on the machining of Al/SiC particulate composites. *Mater Des* 2007;28(5):1584–91.
- [6] Hashim J, Looney L, Hashmi M. Particle distribution in cast metal matrix composites—Part I. *J Mater Process Technol* 2002;123(2):251–7.
- [7] Ozben T, Kilickap E, Cakir O. Investigation of mechanical and machinability properties of SiC particle reinforced Al-MMC. *J Mater Process Technol* 2008;198(1–3):220–5.
- [8] Pawar P, Utpat AA. Development of aluminium based silicon carbide particulate metal matrix composite for spur gear. *Proc Mater Sci* 2014;6:1150–6.
- [9] Sahin Y. Preparation and some properties of SiC particle reinforced aluminium alloy composites. *Mater Des* 2003;24(8):671–9.
- [10] Kwak J, Kim Y. Mechanical properties and grinding performance on aluminum-based metal matrix composites. *J Mater Process Technol* 2008;201(1–3):596–600.
- [11] Zhong Z. Grinding of aluminium-based metal matrix composites reinforced with Al<sub>2</sub>O<sub>3</sub> or SiC particles. *Int J Adv Manuf Technol* 2003;21(2):79–83.
- [12] Pérez-Bustamante R, et al. Microstructural and mechanical characterization of Al-MWCNT composites produced by mechanical milling. *Mater Sci Eng A* 2009;502(1–2):159–63.
- [13] Reddy NSK, Kwang-Sup S, Yang M. Experimental study of surface integrity during end milling of Al/SiC particulate metal-matrix composites. *J Mater Process Technol* 2008;201(1–3):574–9.
- [14] Kuram E, Ozcelik B. Multi-objective optimization using Taguchi based grey relational analysis for micro-milling of Al 7075 material with ball nose end mill. *Measurement* 2013;46(6):1849–64.
- [15] Said MS, et al. Optimisation of end milling machining parameters using the Taguchi method and ANOVA of AlSi/AlN metal matrix composite material. *Key Eng Mater* 2016;701:200–4.
- [16] Magibalan S, Prabu M, Vignesh P. Experimental study on the cutting surface roughness in CNC turning operations by using TAGUCHI technique. *J Chem Pharmaceut Sci* 2015;2:115, www.jchps.com. ISSN: 974.
- [17] Sarkaya M, Yılmaz V, Güllü A. Analysis of cutting parameters and cooling/lubrication methods for sustainable machining in turning of Haynes 25 superalloy. *J Clean Prod* 2016;133:172–81.
- [18] Yıldırım ÇV, et al. Determination of MQL parameters contributing to sustainable machining in the milling of nickel-base superalloy waspalo. *Arab J Sci Eng* 2017;42(11):4667–81.
- [19] Karabulut Ş, Gökmen U, Çinicı H. Optimization of machining conditions for surface quality in milling AA7039-based metal matrix composites. *Arab J Sci Eng* 2018;43(3):1071–82.